Metamaterial thermal emitters based on nanowire cavities for high-efficiency thermophotovoltaics



2014 J. Opt. 16 035102

(http://iopscience.iop.org/2040-8986/16/3/035102)

IOP Publishing Journal of Optics
J. Opt. **16** (2014) 035102 (6pp) doi:10.1088/2040-8978/16/3/035102

# Metamaterial thermal emitters based on nanowire cavities for high-efficiency thermophotovoltaics

**Huixu Deng, Tianchen Wang, Jie Gao and Xiaodong Yang**

Department of Mechanical and Aerospace Engineering, Missouri University of Science and Technology, Rolla, MO 65409, USA

E-mail: yangxia@mst.edu

Received 16 September 2013, in final form 22 December 2013
Accepted for publication 2 January 2014
Published 3 February 2014

**Abstract**

Metamaterial thermal emitters based on gold nanowire cavities on a gold substrate are designed to achieve a narrowband emission spectrum with the emission peak located slightly above the bandgap of photovoltaic (PV) cells, in order to improve the overall efficiency of thermophotovoltaic (TPV) systems. The metamaterial emitter made of gold nanowires embedded in an alumina host exhibits an effective permittivity with extreme anisotropy, which supports cavity resonant modes of both electric dipole and magnetic dipole. The impedance match between the cavity modes and free space leads to strong thermal emission with the desired frequency range slightly above the bandgap of PV cells. Simulation results show that the designed metamaterial emitters are polarization-insensitive and have nearly omnidirectional emission angles. Moreover, theoretical analysis predicts that the overall efficiency of the TPV system can reach Shockley–Queisser limit at a low emitter temperature of $T_e = 940$ K.

Keywords: metamaterials, thermal emitter, thermophotovoltaics
PACS numbers: 78.67.Pt, 78.20.nd, 44.40.+a, 79.60.Jv, 78.67.Uh

(Some figures may appear in colour only in the online journal)

## 1. Introduction

Metamaterials with artificial structured composites can exhibit intriguing electromagnetic phenomena, such as negative refraction [1], invisible cloaking [2], near-zero permittivity [3], and indefinite cavities [4, 5]. The macroscopic properties of metamaterials can be tailored flexibly by designing the artificial meta-atoms. Metamaterial absorbers and emitters working at THz and infrared frequency range have been designed and demonstrated recently [6–12], which hold great promise in light harvesting, thermal detection and electromagnetic energy conversion. In the application of thermal energy harvesting using photovoltaic (PV) cells, the main challenge is to improve the efficiency of thermophotovoltaic (TPV) systems in which the energy conversion process is from heat to electricity via photons as shown in figure 1(a). The maximum efficiency is defined by Shockley–Queisser (SQ) limit, which arises mainly from two loss mechanisms: on one hand, photons incident on the PV cells with energy lower than the PV cell bandgap energy will not be absorbed by the PV cell and lost in free space; on the other hand, photons with energy above the bandgap energy can be absorbed, but the excess energy will be lost in generating undesirable heat. An effective way to avoid these two kinds of loss is to design a thermal emitter with resonance frequency located slightly above the PV cell bandgap energy and narrow emission spectrum bandwidth.

Recently, many efforts have focused on designing metamaterial thermal emitters based on the spectrally selective perfect absorption [13–16] since the absorption spectrum is the same as the emission spectrum for the structures due to Kirchhoff's law. Wu *et al* [17] presented the concept of solar absorber/narrowband thermal emitter (SANTE) based

 

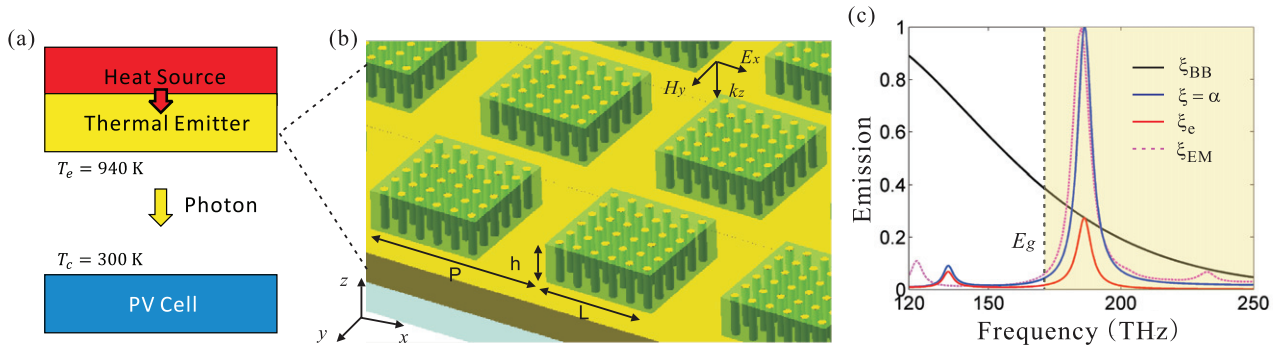


**Figure 1.** Schematic of the TPV system and the emission spectra of the metamaterial emitter. (a) The TPV system mainly includes three components: the heat source to provide thermal energy, the thermal emitter to emit photons at specific frequency and the PV cell to collect photons and generate electricity. (b) The structure of the metamaterial thermal emitter made of gold nanowires embedded in an alumina host. (c) The simulated emission spectra where the yellow area is above the bandgap and represents the photons that can be absorbed by the PV cell.

on integrating broad-band solar radiation absorption with selective narrow-band thermal IR radiation which can be efficiently coupled to a PV cell for power generation. The overall efficiency of this designed system can exceed the SQ limit for emitter temperatures above 1200 K, and even achieve an efficiency as high as 41% for 2300 K. And Molesky *et al* [18] also demonstrated a method for engineering thermally excited far field electromagnetic radiation using high temperature epsilon-near-zero and epsilon-near-pole metamaterial emitters, which can be also used as part of TPV devices to surpass the SQ limit near 1500 K. In addition, extensive work on nanowire metamaterial and radiative heat transfer for TPV applications has been done. Nefedov *et al* [19] proposed a different paradigm of the radiation heat transfer, which makes possible the giant radiative heat transfer for micro-thick gaps based on the structures containing arrays of nanotubes or nanowires. Simovski *et al* [20] also demonstrated the optimal design of the radiative heat transfer in micro-thick multilayer stacks of metamaterials with hyperbolic dispersion for prospective TPV systems by taking into account high temperatures of the emitting medium and the heating of the PV medium by the low-frequency part of the radiation spectrum. Furthermore, since most of the designed emitters for TPV systems operate at high temperatures (>1000 K), structures were usually designed by selecting proper materials to prevent melting, evaporation or chemical reaction and also by maintaining structural stability to avoid thermo-mechanical problems [21]. Thus, a metamaterial thermal emitter operating at a low temperature indicates potential applications in TPV systems by extending the material selection and getting rid of the aforementioned problems at high temperature.

In this paper, a thermal emitter based on metamaterial nanowire cavities is investigated in order to make it work at a low temperature as well as to improve the overall efficiency of TPV systems. The unit cell of this thermal emitter with a period of $P = 600$ nm is shown in figure 1(b), and consists of two elements: the nanowire cavities array and the 140 nm thick gold substrate as a metallic mirror. The cavity is made of $6 \times 6$ gold nanowires with radius $r_0$ and center-to-center distance $D = 60$ nm embedded in an alumina host which forms a cube with $L = 360$ nm and $h = 140$ nm. To model the thermal emitter in finite-element method simulation, the permittivity of gold is described by Drude model: $\varepsilon_m(\omega) = 1 - \omega_p^2/\omega(\omega + i\gamma_0)$, where $\omega$ is the frequency, $\omega_p = 1.37 \times 10^{16}$ rad s$^{-1}$ is the plasma frequency and $\gamma_0 = 4.08 \times 10^{13}$ rad s$^{-1}$ is the bulk collision frequency, while the permittivity of alumina is $\varepsilon_d = 3.0625$. From the simulation results, the absorption spectrum $\alpha$ can be obtained by $\alpha = 1 - R$ since only the reflection spectrum $R$ can be calculated in simulation and the transmission is zero due to the thick gold substrate. In addition, according to Kirchhoff's law of thermal radiation, at thermal equilibrium, the absorption is equal to the emission, $\xi = \alpha$, for every frequency, direction and polarization. Thus, the emission behaviors of the thermal emitter can be unveiled based on the absorption spectrum.

The emission spectrum of the thermal emitter is shown as the blue curve in figure 1(c), where the radius of the nanowire is $r_0 = 12.5$ nm and normal incidence is applied. It can be seen that the main emission peak of almost 100% is achieved at the frequency of 187 THz (corresponding to 0.77 eV). The normalized emission spectrum of ideal blackbody $\xi_{BB}$ is also presented as the black curve in figure 1(c) at the temperature of $T = 940$ K. And the thermal emissivity of the emitter $E_e$ at $T = 940$ K can be obtained by $E_e = \xi_{BB} \times \xi$ as the red curve in figure 1(c). The nanowire cavity can be also regarded as an anisotropic medium according to the effective medium theory (EMT) with the following permittivity components [22],

$$\begin{aligned} \varepsilon_x = \varepsilon_y &= \varepsilon_d \frac{(1+f_m)\varepsilon_m + (1-f_m)\varepsilon_d}{(1-f_m)\varepsilon_m + (1+f_m)\varepsilon_d}, \\ \varepsilon_z &= f_m\varepsilon_m + (1-f_m)\varepsilon_d \end{aligned} \tag{1}$$

where $f_m = \pi r_0^2/D^2$ is the volume filling ratio of gold nanowires. As shown in figure 1(c), the emission spectrum computed by EMT, $\xi_{EM}$, is almost the same as that of the realistic nanowire structures, $\xi$. The slight shift of emission peaks is attribute to the weak nonlocal effects [23].

## 2. Analysis of the thermal emitter

In order to gain further insight into how the nanowire cavity enhances the thermal emission, the electric and magnetic

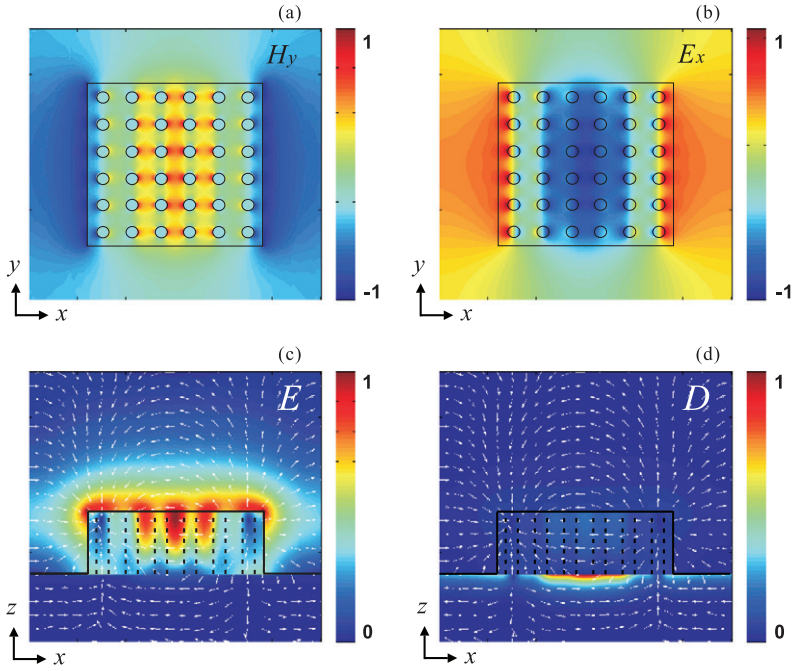


**Figure 2.** (a) and (b) are the magnetic field profile and the electric field profile of the nanowire cavity in the $x$–$y$ plane, respectively. (c) The intensity and direction of the electric field distribution and (d) the displacement current distribution in the $x$–$z$ plane.

fields in the structure are simulated by finite element method, which is excited by a normally incident plane wave at the resonant frequency. Figures 2(a) and (b) show the magnetic field profile $H_y$ and the electric field profile $E_x$ in the $x$–$z$ plane, respectively. The mechanism of high emission for the thermal emitter on resonance can be understood as the cavity supports electric dipole resonance and magnetic dipole resonance simultaneously. The electric dipole resonance can be observed from the accumulation of polarized positive charges and negative charges at the top left and top right corners of the cavity (figure 2(c)) by calculating the divergence of the electric field ($\nabla \cdot \mathbf{E} = \rho/\varepsilon_0$, where $\rho$ is the polarized charge density). Additionally, the magnetic dipole resonance can be seen from the anti-parallel displacement current ($\partial D/\partial t = -\mathrm{i}\omega D = -\mathrm{i}\omega\varepsilon E$, figure 2(d)) formed between the nanowire cavity and the gold substrate due to the large negative permittivity of metal.

To analyze the high emission on resonance quantitatively, effective permittivity and permeability of the structure are retrieved to obtain the impedance, by using the method described by [24] from which the condition of impedance match to the free space can be achieved. With the calculated reflection ($S_{11}$) and transmission ($S_{21}$), the impedance $z$ can be written as:

$$z = \sqrt{\frac{\mu_{\mathrm{eff}}}{\varepsilon_{\mathrm{eff}}}} = \pm\sqrt{\frac{(1+S_{11})^2 - S_{21}^2}{(1-S_{11})^2 - S_{21}^2}}. \qquad (2)$$

At the resonance of cavity mode, $z = 0.976 + 0.017\mathrm{i}$, which perfectly match the free space impedance $z_0$. The corresponding effective permittivity and permeability are $\varepsilon_{\mathrm{eff}} = 0.638 + 2.850\mathrm{i}$ and $\mu_{\mathrm{eff}} = 0.513 + 2.735\mathrm{i}$, respectively, for the cavity mode shown in figure 2.

To ensure the emission resonant frequency is slightly above the bandgap energy for different PV cells, the geometries of the thermal emitter can be tuned accordingly. In the current design, the cavity height $h$ and the filling ratio $f_m$ are tuned to adjust both the resonant frequency position and the impedance match condition, in order to achieve high-efficiency TPV system. Figures 3(b) and (c) show the dependence of emission spectra on the cavity height $h$ and the filling ratio $f_m$ at normal incidence ($\theta = 0°$), respectively. To optimize the TPV system efficiency, the cavity height $h = 140$ nm and the filling ratio $f_m = 14\%$ are used for the PV cell of GaSb (with the bandgap energy of $E_{\mathrm{g}} = 0.71$ eV). Note that the nanowire cavity can be designed for different PV cells with certain bandgap energy by simply tuning the cavity geometry.

Furthermore, the designed thermal emitter is polarization-insensitive and nearly omnidirectional for all the emission angles (figure 3(a)). It is polarization-independent since the nanowire cavity possesses 4-fold rotation symmetry in the $x$–$y$ plane. For oblique incidence, the emission spectra of both polarizations (transverse electric (TE) polarization and transverse magnetic (TM) polarization) are almost the same so that the average of both the TE and TM emission spectra, $\xi = (\xi_{\mathrm{TE}} + \xi_{\mathrm{TM}})/2$, is taken as the actual emission of the thermal emitter as shown in figure 3(d). As the emission angle increases up to 80° for both TE and TM, the frequency of emission peak remains the same and the emission strength always keeps at a high level.

## 3. Efficiency of the TPV system

To evaluate the performance of the metamaterial thermal emitter made of nanowire cavities for TPV systems, the overall

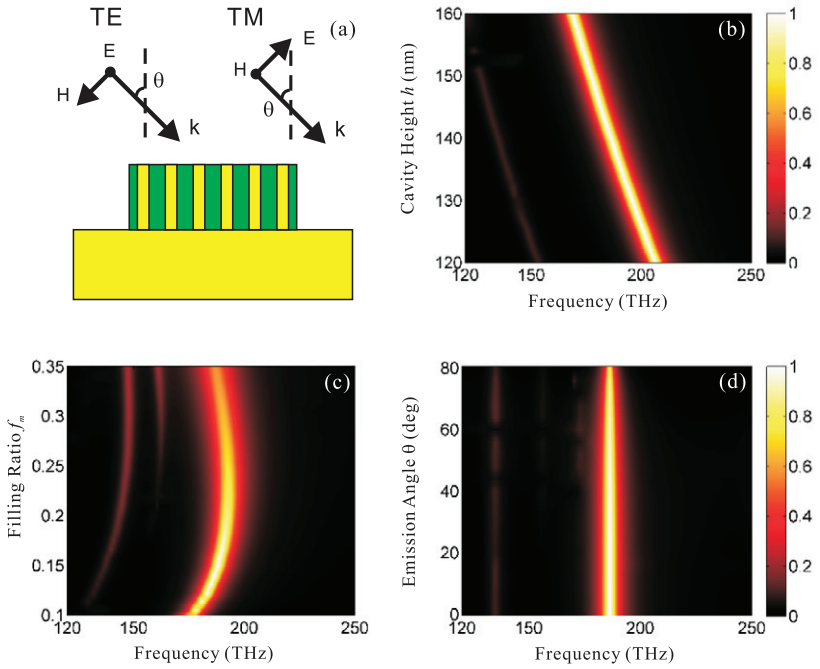


**Figure 3.** (a) The configurations of TE and TM polarization. (b) and (c) show the dependence of emission spectra on the cavity height $h$ and the metal filling ratio $f_m$ at normal emission angle ($\theta = 0°$), respectively. (d) The average of both the TE and TM emission spectra, $\xi = (\xi_{TE} + \xi_{TM})/2$, which is taken as the actual emission of the thermal emitter.

system efficiency is theoretically calculated. In general, the maximum efficiency of a system is limited by the Carnot efficiency (all heat energy is converted to electrical energy without loss) which can be given by $\eta_{car} = 1 - T_c/T_e$. When the temperature of the PV cell collector $T_c$ is 300 K and the temperature of the emitter $T_e$ is maintained at 1000 K, a maximum efficiency of 70% can be obtained. However, for TPV systems, efficiencies are limited by other factors in the energy conversion process from heat to electricity via photons. Following the analysis by Shockley and Queisser, the overall energy conversion efficiency of TPVs is [13, 17, 25]:

$$\eta = U(T, E_g) \times \nu(T, E_g) \times m(V_{op}). \tag{3}$$

In this equation, $U$ is the ultimate efficiency related to the photon absorption process by the PV cell and proportional to the energy contained in photon-excited electron–hole pairs divided by the incident radiation energy. Besides, $\nu$ and $m$ are related to the energy transfer process inside the PV cell. $\nu$ is an efficiency due to recombination process of charge carriers, which means charge carriers may be removed from the PV cell in additional ways. And $m$ is called impedance mismatch efficiency caused by the difference between the open circuit voltage $V_{op}$ and the optimal operating voltage in the PV cell.

According to the assumption that one photon with energy larger than the PV cell bandgap energy $E_g$ will excite one electron–hole pair resulting in the contribution of $E_g$ electricity energy to the TPV system, the ultimate efficiency can be achieved by calculating the energy carried by excited electron–hole pairs with respect to the incident radiation energy [13, 17, 18]:

$$U = \frac{\int_0^{\pi/2} d\theta \, \sin(2\theta) \int_{E_g}^{\infty} dE \, \xi(E,\theta) I_{BB}(E, T_e) \frac{E_g}{E}}{\int_0^{\pi/2} d\theta \, \sin(2\theta) \int_0^{\infty} dE \, \xi(E,\theta) I_{BB}(E, T_e)}. \tag{4}$$

In this equation, the denominator is the incident radiation energy onto the PV cell, which is equal to the thermal emission energy from the emitter calculated by the integral of blackbody radiation $I_{BB}$ (when the emitter temperature is $T_e$) multiplying the emission of the emitter at all emission angles $\theta$ (assuming the emitter to be planar with no azimuthal angular dependence). The numerator is the energy contained in excited electron–hole pairs by cutting off the photon energy below $E_g$ and reducing the higher photon energy into $E_g$. In order to average the emission in both TE and TM polarizations, $\xi(E,\theta) = \xi_{TE}(E,\theta)/2 + \xi_{TM}(E,\theta)/2$ is considered.

Besides the efficiency of creating excited electron–hole pairs, the recombination efficiency $\nu$ is utilized to measure the per cent of charge carriers becoming the desired external current. And it can be expressed as the ratio between the open circuit voltage $V_{op}$ and the initial material bandgap voltage $V_g = E_g/q$, in which $q$ is the charge of one electron [13, 17]:

$$\nu = \frac{V_{op}}{V_g} = \frac{V_c}{V_g} \ln\left(f \frac{Q_e(T, E_g)}{Q_c(T_c, E_g)}\right) \tag{5}$$

where $V_c = k_B T_c/q$ is the voltage of the PV cell related to the cell temperature $T_c$. $Q_e$ and $Q_c$ are photon number flux incident on the PV cell from the emitter, and from an ideal blackbody surrounding the cell at the same temperature of the PV cell $T_c$, respectively [13, 17]. Here, $f$ is chosen as 0.5 for

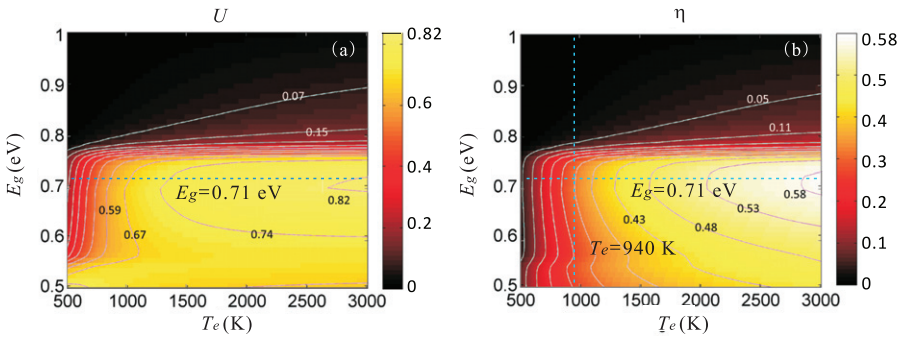


**Figure 4.** Theoretical calculation of the TPV system efficiency as a function of the PV cell bandgap energy $E_g$ and the emitter temperature $T_e$. (a) The ultimate efficiency $U$, where the dashed line represents the bandgap energy of GaSb with $E_g = 0.71$ eV. (b) The overall conversion efficiency, $\eta = U \times \nu \times m$, which can reach the SQ limit of 0.31 when the PV cell is GaSb and the emitter temperature is relatively low at $T_e = 940$ K (represented by the vertical dashed line).

an ideal case when both the emitter and the cell have planar geometries.

The third factor in equation (3), $m(V_{op})$, is evaluated when the operating voltage $V_{max}$ is chosen to maximize the electrical power for the PV cell [13, 17],

$$m(V_{op}) = \frac{z_m^2}{(1 + z_m - e^{-z_m})(z_m + \ln(1 + z_m))} \quad (6)$$

with $z_m$ determined by the ratio between $V_{max}$ and $V_c$ and related to $V_{op}/V_c = z_m + \ln(1 + z_m)$.

When the filling ratio of nanowire is $f_m = 0.14$, each efficiency factor in equation (3), $U$, $\nu$ and $m$, is calculated as functions of the PV cells bandgap energy $E_g$ and the temperature of the emitter $T_e$. $\nu$ and $m$ are both determined by the properties of PV cell. $U$ and $\eta$ are enhanced by the designed thermal emitter as shown in figure 4. The resonant frequency of the emitter is tuned to 187 THz and the emitter temperature is set at about $T_e = 940$ K to reach the SQ limit of $\eta_{SQ} = 0.31$. The emitter temperature required to reach the SQ limit is much lower than the temperature of 2500 K in current existing solar TPV systems. If the temperature is too low, the efficiency will be reduced due to the decrease of $\nu$ and $m$. When the temperature increases, the efficiency can even get higher and exceed the SQ limit, but it is limited by the melting point of the emitter materials [18]. The melting temperature of gold is around 1337 K, which is much higher than the current operation emitter temperature of 940 K. In the future, new design of emitters with high melting point materials can improve the overall efficiency furthermore.

## 4. Conclusions

In conclusion, to improve the overall efficiency of TPV system, a metamaterial thermal emitter based on nanowire cavities is proposed and demonstrated. The cavity mode supports both the electric dipole resonance and the magnetic dipole resonance simultaneously. At the resonant frequency, the impedance of the metamaterial thermal emitter can match the impedance of the free space, resulting in high emissivity with narrow emission bandwidth. The resonant frequency can be tuned to match the bandgap energy of different PV cells by changing the cavity height as well as the filling ratio of gold nanowires. The emission as a function of different angles for both the TE and TM polarizations is also investigated for determining the efficiency of TPV systems. By tuning the emission frequency slightly above the bandgap energy of PV cell, the overall efficiency can reach SQ limit of $\eta_{SQ} = 0.31$ at a low emitter temperature of 940 K. When the emitter temperature is increased, the efficiency can exceed the SQ limit, but it is still limited by the melting point of the emitter materials.

## Acknowledgments

This work was partially supported by the Intelligent Systems Center and the Energy Research and Development Center at Missouri S&T, the University of Missouri Interdisciplinary Intercampus Research Program, and the University of Missouri Research Board. The authors acknowledge Y He for helpful discussions about this work.

## References

[1] Shelby R A, Smith D R and Schultz S 2001 Experimental verification of a negative index of refraction *Science* **292** 77–9

[2] Pendry J B, Schurig D and Smith D R 2006 Controlling electromagnetic fields *Science* **312** 1780–2

[3] Alù A, Silveirinha M G, Salandrino A and Engheta N 2007 Epsilon-near-zero metamaterials and electromagnetic sources: tailoring the radiation phase pattern *Phys. Rev.* B **75** 155410

[4] Yang X, Yao J, Rho J, Yin X and Zhang X 2012 Experimental realization of three-dimensional indefinite cavities at the nanoscale with anomalous scaling laws *Nature Photon.* **6** 450–4

[5] Yao J, Yang X, Yin X, Bartal G and Zhang X 2011 Three-dimensional nanometer-scale optical cavities of indefinite medium *Proc. Natl Acad. Sci. USA* **108** 11327–31

[6] Tao H, Landy N I, Bingham C M, Zhang X, Averitt R D and Padilla W J 2008 A metamaterial absorber for the terahertz regime: design, fabrication and characterization *Opt. Express* **16** 7181–8

[7] Liu N, Mesch M, Weiss T, Hentschel M and Giessen H 2010 Infrared perfect absorber and its application as plasmonic sensor *Nano Lett.* **10** 2342–8

[8] Avitzour Y, Urzhumov Y A and Shvets G 2009 Wide-angle infrared absorber based on a negative-index plasmonic metamaterial *Phys. Rev.* B **79** 045131
[9] Liu X, Tyler T, Starr T, Starr A F, Jokerst N M and Padilla W J 2011 Taming the blackbody with infrared metamaterials as selective thermal emitters *Phys. Rev. Lett.* **107** 045901
[10] Cui Y, Fung K H, Xu J, Ma H, Jin Y, He S and Fang N X 2012 Ultrabroadband light absorption by a sawtooth anisotropic metamaterial slab *Nano Lett.* **12** 1443–7
[11] Celanovic I, Perreault D and Kassakian J 2005 Resonant-cavity enhanced thermal emission *Phys. Rev.* B **72** 075127
[12] He Y, Deng H, Jiao X, He S, Gao J and Yang X 2013 Infrared perfect absorber based on nanowire metamaterial cavities *Opt. Lett.* **38** 1179–81
[13] Rephaeli E and Fan S 2009 Absorber and emitter for solar thermo-photovoltaic systems to achieve efficiency exceeding the Shockley–Queisser limit *Opt. Express* **17** 15145–59
[14] Mason J A, Smith S and Wasserman D 2011 Strong absorption and selective thermal emission from a midinfrared metamaterial *Appl. Phys. Lett.* **98** 241105
[15] D'Aguanno G, Mattiucci N, Alù A, Argyropoulos C, Foreman J V and Bloemer M J 2012 Thermal emission from a metamaterial wire medium slab *Opt. Express* **20** 9784–9
[16] Shu S, Zheng L, Li H, Tsang C K, Shi L and Li Y Y 2012 Porous metal-based multilayers for selective thermal emitters *Opt. Lett.* **37** 4883–5
[17] Wu C, Neuner B III, John J, Milder A, Zollars B, Savoy S and Shvets G 2012 Metamaterial-based integrated plasmonic absorber/emitter for solar thermo-photovoltaic systems *J. Opt.* **14** 024005
[18] Molesky S, Dewalt C J and Jacob Z 2013 High temperature epsilon-near-zero and epsilon-near-pole metamaterial emitters for thermophotovoltaics *Opt. Express* **21** A96–110
[19] Nefedov I S and Simovski C R 2011 Giant radiation heat transfer through micron gaps *Phys. Rev.* B **84** 195459
[20] Simovski C, Maslovski S, Nefedov I and Tretyakov S 2013 Optimization of radiative heat transfer in hyperbolic metamaterials for thermophotovoltaic applications *Opt. Express* **21** 14988–5013
[21] Yeng Y X, Ghebrebrhan M, Bermel P, Chan W R, Joannopoulos J D, Soljačić M and Celanovic I 2012 Enabling high-temperature nanophotonics for energy applications *Proc. Natl Acad. Sci. USA* **109** 2280–5
[22] Sihvola A H 1999 *Electromagnetic Mixing Formulae and Applications* (London: Institution of Electrical Engineers)
[23] Elser J, Podolskiy V A, Salakhutdinov I and Avrutsky I 2007 Nonlocal effects in effective-medium response of nanolayered metamaterials *Appl. Phys. Lett.* **90** 191109
[24] Chen X, Grzegorczyk T M, Wu B-I, Pacheco J Jr and Kong J A 2004 Robust method to retrieve the constitutive effective parameters of metamaterials *Phys. Rev.* E **70** 016608
[25] Shockley W and Queisser H J 1961 Detailed balance limit of efficiency of p–n junction solar cells *J. Appl. Phys.* **32** 510–9